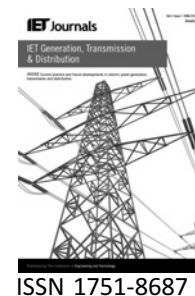


Published in IET Generation, Transmission & Distribution  
 Received on 21st September 2009  
 Revised on 13th January 2010  
 doi: 10.1049/iet-gtd.2009.0533



# Precise fault location algorithm for double-circuit transmission lines using unsynchronised measurements from two anti-parallel ends

G.N. Korres C.A. Apostolopoulos

Electrical and Computer Engineering Department, National Technical University of Athens, Iroon Polytechniou 9, Zografou 15780, Athens, Greece  
 E-mail: apostolo@power.ece.ntua.gr

**Abstract:** A new fault location algorithm for double-circuit transmission lines with availability of complete measurements from two anti-parallel end of the line is presented. Sequence voltage and current phasors from these ends are taken as inputs and no synchronisation between them is needed. Using the pre-fault data, the synchronisation angles between measurements at the reference and the anti-parallel ends are obtained. Using the fault data, the faulted circuit is determined and the sequence voltages and currents at the fault point are calculated as a function of the fault distance. Finally, using the fault boundary conditions that exist for a given fault type, the fault location is derived and solved by an iterative method. Owing to zero-sequence mutual coupling, it is not straightforward to express the zero-sequence voltage and current at the fault point as a function of the zero-sequence voltages and currents at the two measuring ends and the distance to fault. To overcome this problem, a modal transformation matrix is introduced to obtain the modal networks, which are decoupled and can be analysed independently. Based on distributed parameter line model, the proposed algorithm fully considers the effects of shunt capacitances and thus achieves superior locating accuracy, especially for long lines. Mutual coupling between circuits, source impedances and fault resistance do not influence the locating accuracy of the algorithm. The simulation results using ATP-EMTP and MATLAB demonstrate the effectiveness and accuracy of the proposed algorithm.

## 1 Introduction

Double-circuit transmission lines have been extensively utilised in modern power systems to enhance the reliability and security for the transmission of electrical energy. They are usually spreading over few hundreds of kilometres and are vital links between the energy production and consumption centres. The different topologies of double-circuit lines combined with the mutual coupling effect create a large number of possible fault types that may occur on double-circuit lines. This feature makes their protection and fault location determination a very challenging problem.

Many fault location algorithms for double-circuit lines have been developed [1–11]. These algorithms are based

on either one-terminal [1–7] or two-terminal data [8–11]. Although less precise than two-terminal algorithms, one-terminal algorithms appear more attractive since they rely only on voltage and current measurements at one common terminal, and hence no communication links have to be provided between both terminals of the line. One-terminal data algorithms [1–6] are based on lumped parameter line model. While different in their implementation issues, these algorithms attempt to estimate the fault current contribution from the other terminal by solving the Kirchhoff's voltage law (KVL) equations around parallel lines loops. Since they are based on lumped parameter line model, these algorithms do not fully consider the shunt capacitance effect. This may lead to significant errors in fault location estimation, especially for long lines where the magnitude of the capacitive

charging current can be comparable to the fault current, particularly under high impedance fault conditions. Moreover, none of these algorithms deals effectively with inter-circuit faults which are more likely to occur on double-circuit lines located on the same tower structure. Recently, a one-terminal algorithm based on distributed parameter line model has been developed [7], having high locating accuracy and treating satisfactorily most of the asymmetrical fault types that can be encountered in double-circuit lines. However, it cannot be used to locate symmetrical faults between circuits, for example, a fault involving phases A and B in both circuits of the line at the same instant.

Contrary to one-terminal algorithms, there are few two-terminal algorithms for double-circuit lines [8–11]. Voltage and current measurements from all four measuring ends of a double-circuit line are considered in [8]. Although the algorithm is based on distributed parameter line model and is capable of locating inter-circuit faults, it requires a great amount of data to be transferred from all line ends. There is also one two/multi-terminal algorithm based on lumped parameter line model [9] and two other algorithms based on distributed parameter line model [10, 11]. These last two algorithms utilise only current measurements from all four ends of the line, which adversely affects their accuracy due to current transformers' (CTs) errors.

This paper presents a new fault location algorithm for double-circuit transmission lines that is based only on voltage and current measurements at two anti-parallel ends of the line. Using a limited number of measurements, the proposed algorithm manages to reduce the amount of information needed to be exchanged between the line terminals to estimate the distance to fault. Furthermore, comparing to [10, 11] the algorithm is more secure since it is not so highly affected by CT errors. Finally, although the proposed algorithm does not require synchronisation between measurements at the two measuring ends, it can also be applied in a fault location scheme with utilisation of synchronised phasor measurement units (PMUs). In such a scheme, the proposed algorithm offers minimal PMU placement for locating faults in double-circuit lines, which is considered as a very useful add-on in an attempt to achieve transmission network fault location observability with minimum number of PMUs [12].

The rest of the paper is organised as follows. Section 2 presents a modal transformation to decouple the six-phase system of a double-circuit transmission line into positive, negative and zero-sequence networks [13]. Assuming that the line is well transposed, the equivalent PI circuit of positive and negative sequence networks, based on distributed parameter line model, can be readily accomplished. Owing to mutual coupling, it is not straightforward to obtain the equivalent PI circuit for zero-sequence networks. However, using the proposed modal

transformation matrix, the zero-sequence networks can be decoupled into common and differential component networks [7], which can be analysed independently. Section 3 presents the basic background of the proposed algorithm, comprising the following critical tasks: phasor computation, synchronisation error determination, fault-type detection, faulted circuit selection and fault location estimation. Using the fundamental sequence voltage and current phasors from the two measuring ends, in combination with the equivalent PI circuits of the sequence networks derived in Section 2, the sequence voltages and currents at the fault location can be expressed as a function of the fault distance only. Thereafter, applying the fault boundary conditions that exist for each fault type, the fault location can be determined by using a numerical method. In Section 4, detailed alternative transient program (ATP) and MATLAB simulation results are presented to demonstrate the effectiveness and accuracy of the proposed method.

## 2 Derivation of equivalent PI circuit for sequence networks of a double-circuit line

The objective is to derive an equivalent PI circuit for positive, negative and zero-sequence networks of a double-circuit line, accounting for distributed parameter effects. This will ensure precision of the results obtained by the proposed fault location algorithm. Double-circuit transmission lines involve two parallel circuits. Fig. 1 shows a typical tower and conductor configuration of a double-circuit line. Considering the coupling between conductors and assuming that the two circuits of the line have identical parameters and are well-transposed, the voltages and currents along the line satisfy the following equation [14]

$$\begin{cases} \frac{d[V_{\text{phase}}]}{dx} = [Z_{\text{phase}}][I_{\text{phase}}] \\ \frac{d[I_{\text{phase}}]}{dx} = [Y_{\text{phase}}][V_{\text{phase}}] \end{cases} \quad (1)$$

where  $[V_{\text{phase}}] = [V_{a-I}; V_{b-I}; V_{c-I}; V_{a-II}; V_{b-II}; V_{c-II}]^T$  and  $[I_{\text{phase}}] = [I_{a-I}; I_{b-I}; I_{c-I}; I_{a-II}; I_{b-II}; I_{c-II}]^T$  are the phase

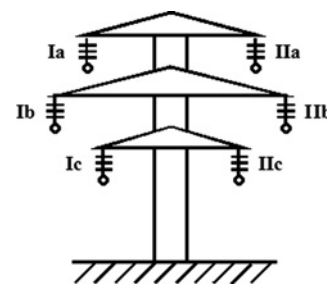


Figure 1 Structure of a double-circuit transmission line

voltage and current vectors of circuits I and II at considered point, respectively;  $[Z_{\text{phase}}]$  and  $[Y_{\text{phase}}]$  are the phase series impedance and shunt admittance matrices given as

$$[Z_{\text{phase}}] = \begin{pmatrix} Z_s & Z_m & Z_m & Z_p & Z_p & Z_p \\ Z_m & Z_s & Z_m & Z_p & Z_p & Z_p \\ Z_m & Z_m & Z_s & Z_p & Z_p & Z_p \\ Z_p & Z_p & Z_p & Z_s & Z_m & Z_m \\ Z_p & Z_p & Z_p & Z_m & Z_s & Z_m \\ Z_p & Z_p & Z_p & Z_m & Z_m & Z_s \end{pmatrix}$$

$$[Y_{\text{phase}}] = \begin{pmatrix} Y_s & Y_m & Y_m & Y_p & Y_p & Y_p \\ Y_m & Y_s & Y_m & Y_p & Y_p & Y_p \\ Y_m & Y_m & Y_s & Y_p & Y_p & Y_p \\ Y_p & Y_p & Y_p & Y_s & Y_m & Y_m \\ Y_p & Y_p & Y_p & Y_m & Y_s & Y_m \\ Y_p & Y_p & Y_p & Y_m & Y_m & Y_s \end{pmatrix} \quad (2)$$

where  $Z_s$ ,  $Z_m$  and  $Y_s$ ,  $Y_m$  are the self and mutual coupling impedances and admittances, respectively, associated with either one circuit taken separately;  $Z_p$  and  $Y_p$  is the mutual coupling impedance and admittance between any one of three conductors of one circuit and any one of the three conductors of the other circuit.

Using eigenvalue theory [15], the line parameter matrices  $[Z_{\text{phase}}]$  and  $[Y_{\text{phase}}]$  can be decoupled into diagonal matrices. The modal transformation matrices for voltage and current  $[T_v]$  and  $[T_i]$  can be used for diagonalisation. Then, (1) can be written as

$$\begin{cases} \frac{d[V_{\text{mode}}]}{dx} = [T_v]^{-1}[Z_{\text{phase}}][T_i][I_{\text{mode}}] = [Z_{\text{mode}}][I_{\text{mode}}] \\ \frac{d[I_{\text{mode}}]}{dx} = [T_i]^{-1}[Y_{\text{phase}}][T_v][V_{\text{mode}}] = [Y_{\text{mode}}][V_{\text{mode}}] \end{cases} \quad (3)$$

where  $[V_{\text{mode}}] = [T_v]^{-1}[V_{\text{phase}}] = [V_{1-I}; V_{2-I}; V_{1-II}; V_{2-II}; 1/2(V_{0-II} - V_{0-I}); 1/2(V_{0-I} + V_{0-II})]^T$  and  $[I_{\text{mode}}] = [T_i]^{-1}[I_{\text{phase}}] = [I_{1-I}; I_{2-I}; I_{1-II}; I_{2-II}; 1/2(I_{0-II} - I_{0-I}); 1/2(I_{0-I} + I_{0-II})]^T$  are the modal voltage and current vectors expressed with respect to the sequence voltages and currents of circuits I and II at considered point and

$$T_v = T_i = \begin{pmatrix} 1 & 1 & 0 & 0 & -1 & 1 \\ a^2 & a & 0 & 0 & -1 & 1 \\ a & a^2 & 0 & 0 & -1 & 1 \\ 0 & 0 & 1 & 1 & 1 & 1 \\ 0 & 0 & a^2 & a & 1 & 1 \\ 0 & 0 & a & a^2 & 1 & 1 \end{pmatrix}, \quad T_v^{-1} = T_i^{-1}$$

$$= \begin{pmatrix} (1/3) & (1/3)a & (1/3)a^2 & 0 & 0 & 0 \\ (1/3) & (1/3)a^2 & (1/3)a & 0 & 0 & 0 \\ 0 & 0 & 0 & (1/3) & (1/3)a & (1/3)a^2 \\ 0 & 0 & 0 & (1/3) & (1/3)a^2 & (1/3)a \\ -1/6 & -1/6 & -1/6 & 1/6 & 1/6 & 1/6 \\ 1/6 & 1/6 & 1/6 & 1/6 & 1/6 & 1/6 \end{pmatrix} \quad (4)$$

where  $a = e^{j120}$ .

In (3),  $[Z_{\text{mode}}]$  and  $[Y_{\text{mode}}]$  are the modal series impedance and shunt admittance matrices that are equal to

$$[Z_{\text{mode}}] = \begin{pmatrix} Z_1 & 0 & 0 & 0 & 0 & 0 \\ 0 & Z_1 & 0 & 0 & 0 & 0 \\ 0 & 0 & Z_1 & 0 & 0 & 0 \\ 0 & 0 & 0 & Z_1 & 0 & 0 \\ 0 & 0 & 0 & 0 & Z_{1L} & 0 \\ 0 & 0 & 0 & 0 & 0 & Z_G \end{pmatrix}$$

$$[Y_{\text{mode}}] = \begin{pmatrix} Y_1 & 0 & 0 & 0 & 0 & 0 \\ 0 & Y_1 & 0 & 0 & 0 & 0 \\ 0 & 0 & Y_1 & 0 & 0 & 0 \\ 0 & 0 & 0 & Y_1 & 0 & 0 \\ 0 & 0 & 0 & 0 & Y_{1L} & 0 \\ 0 & 0 & 0 & 0 & 0 & Y_G \end{pmatrix} \quad (5)$$

where  $Z_1 = Z_s - Z_m$ ,  $Z_0 = Z_s + 2Z_m$ ,  $Z_{M0} = 3Z_p$  and  $Y_1 = Y_s - Y_m$ ,  $Y_0 = Y_s + 2Y_m$ ,  $Y_{M0} = 3Y_p$  are the positive, zero and mutual zero-sequence impedances and admittances of the line, respectively;  $Z_{1L} = Z_0 - Z_{M0}$ ,  $Z_G = Z_0 + Z_{M0}$  and  $Y_{1L} = Y_0 - Y_{M0}$ ,  $Y_G = Y_0 + Y_{M0}$  are the inter-circuit and ground mode impedances and admittances of the line, respectively [16].

In the mode domain, define

$$Z_{c1} = \sqrt{Z_1/Y_1}, \quad \gamma_{c1} = \sqrt{Z_1 Y_1} \quad (6)$$

$$Z_{c0d} = \sqrt{Z_{1L}/Y_{1L}}, \quad \gamma_{c0d} = \sqrt{Z_{1L} Y_{1L}} \quad (7)$$

$$Z_{c0c} = \sqrt{Z_G/Y_G}, \quad \gamma_{c0c} = \sqrt{Z_G Y_G} \quad (8)$$

$$V_{0d} = \frac{1}{2}(V_{0-II} - V_{0-I}), \quad I_{0d} = \frac{1}{2}(I_{0-II} - I_{0-I}) \quad (9)$$

$$V_{0c} = \frac{1}{2}(V_{0-I} + V_{0-II}), \quad I_{0c} = \frac{1}{2}(I_{0-I} + I_{0-II}) \quad (10)$$

where  $Z_{c1}$  and  $\gamma_{c1}$  are the characteristic impedance and propagation constant of positive and negative sequence networks for each line circuit, respectively;  $Z_{c0d}$ ,  $\gamma_{c0d}$  and  $Z_{c0c}$ ,  $\gamma_{c0c}$  are the characteristic impedances and propagation constants of the differential and the common sequence network, that the mutually coupled zero-sequence networks of the double-circuit line are decoupled into, respectively;  $V_{0d}$ ,  $I_{0d}$

and  $V_{0c}$ ,  $I_{0c}$  are the differential and common sequence voltages and currents, respectively.

Based on (3) and Fig. 2, the mode voltages and currents along the line at considered point  $x$  are written as

$$V_{1-j} = V_{s1-j} \cosh(\gamma_{c1}x) - I_{s1-j}Z_{c1} \sinh(\gamma_{c1}x) \quad (11)$$

$$I_{1-j} = I_{s1-j} \cosh(\gamma_{c1}x) - V_{s1-j} \sinh(\gamma_{c1}x)/Z_{c1} \quad (12)$$

$$V_{2-j} = V_{s2-j} \cosh(\gamma_{c1}x) - I_{s2-j}Z_{c1} \sinh(\gamma_{c1}x) \quad (13)$$

$$I_{2-j} = I_{s2-j} \cosh(\gamma_{c1}x) - V_{s2-j} \sinh(\gamma_{c1}x)/Z_{c1} \quad (14)$$

$$V_{0p} = V_{s0p} \cosh(\gamma_{c0p}x) - I_{s0p}Z_{c0p} \sinh(\gamma_{c0p}x) \quad (15)$$

$$I_{0p} = I_{s0p} \cosh(\gamma_{c0p}x) - V_{s0p} \sinh(\gamma_{c0p}x)/Z_{c0p} \quad (16)$$

where  $V_{s1-j}$ ,  $V_{s2-j}$ ,  $V_{s0p}$  and  $I_{s1-j}$ ,  $I_{s2-j}$ ,  $I_{s0p}$  are the modal voltages and currents at terminal  $s_j$ , respectively;  $j = I, II$ , representing the circuits I and II of the line;  $p = d, c$ , standing for the differential and common sequence component. Combining (11)–(16), enables the development of the equivalent PI circuit for particular sequence networks of a double-circuit line, which is the basis for analysing the proposed fault location algorithm. This analysis is given in the following section.

### 3 Fault location algorithm

Fig. 3 shows the proposed measuring arrangement for locating faults in a double-circuit transmission line. Voltages and currents from two anti-parallel ends of the line are used. We assume that the fault locator (FL) is installed at the line end  $s_I$  and is supplied directly with signals from the voltage and current transformers  $VT_{s_S1}$  and  $CT_{s_S1}$ , respectively. In turn, the signals from the instrument transformers  $VT_{s_RII}$  and  $CT_{s_RII}$  at the anti-parallel end  $r_{II}$  are recorded by a digital fault recorder (DFR) and sent via a communication link to the FL. The CTs are connected on the line side of each breaker, thus enabling the algorithm to operate additionally for ground faults that occur while one circuit is in operation and the other is out of service with its ends grounded.

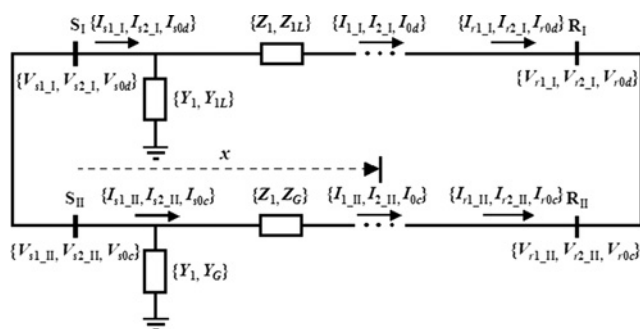


Figure 2 Modal sequence networks of a double-circuit line

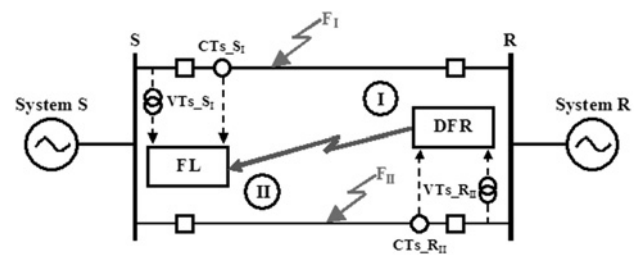


Figure 3 Schematic diagram of the fault location scheme for double-circuit lines

It is to be mentioned that there is no global positioning system (GPS) control of digital measurements performed at the two line ends, and thus, a more general case of unsynchronised measurements, similarly as in [17], is considered. Moreover, fully transposed lines and identical parameters between the circuits of the double-circuit line are assumed, which allows using the theory presented in the previous section.

The proposed fault location algorithm for double-circuit lines comprises the following tasks:

1. phasor estimation, fault-type detection, fault recording segmentation and data alignment;
2. synchronisation error determination, using pre-fault data;
3. faulted circuit selection, using fault data;
4. fault location estimation.

The above-mentioned tasks and their implementation issues are discussed in the following paragraphs.

#### 3.1 Phasor estimation, fault-type detection, fault recording segmentation and data alignment

The proposed algorithm uses only the sequence voltage and current phasors. Thus, the phase voltage and current waveforms captured by the two DFRs must be converted into sequence fundamental frequency phasors. This is accomplished using a three-stage approach. Initially, the phase voltage and current signals are filtered by a low-pass filter to remove possible noise and higher harmonics. Afterwards, the phase voltage and current phasors are calculated with the use of DFT algorithm. Finally, the symmetrical component transformation is applied to obtain the sequence voltages and currents. When fault recordings do not originate from DFRs but are products of digital relays with already calculated signal phasors, the algorithm is still capable of manipulating them via the Comtrade data format [18].

The next step is to identify the fault type and determine the phase(s) involved in the fault. Numerous types of faults

can be encountered in double-circuit lines. Therefore we have implemented a highly secure algorithm [19] for fault-type identification. This algorithm is capable of dealing with both challenging issues of phase selection in double-circuit lines, weak-infeed conditions and inter-circuit faults. Moreover, within the fault-type selection process, we can estimate the individual fault inception timings of the unsynchronised recordings captured at the two measuring ends. Using this information, we can (a) divide the fault recordings into pre-fault and fault segments, (b) time-align the fault recordings, by equating their fault inception times; that is, we choose the recording with the minimum fault inception time as the reference one, and then we left-shift the other recording, until its fault inception time becomes equal to the reference one.

### 3.2 Synchronisation error determination

The fault-type detection algorithm is used to synchronise the signals from both line ends. However, there is still a need to refine synchronisation of phasors, because error with the maximum of one sampling interval is possible after the data alignment phase. For example, if we have one sampling interval shift between two signals and we use 1 kHz sampling frequency, then there will be 18° phase angle difference between the phasors obtained from these signals. The fault location estimation algorithm is sensitive to such phase angle difference and additional effort should be made to achieve better synchronisation. To solve this problem, we can assume balanced operation of the power system preceding the fault and, by employing the positive sequence equivalent PI circuit of the double-circuit line depicted in Fig. 4, we can calculate the phase angle difference between two voltage and current positive sequence phasors at the anti-parallel sides.

In Fig. 4, the following notations are adopted:

$V_{s1-I}, I_{s1-I}$  and  $V_{r1-II}, I_{r1-II}$ : pre-fault positive sequence voltage and current at measuring ends  $s_I$  and  $r_{II}$ , respectively;

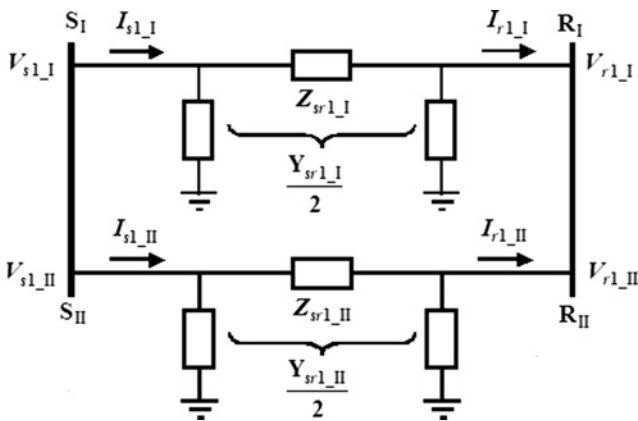


Figure 4 Positive sequence equivalent PI circuit of a double-circuit line

$V_{r1-I}, I_{r1-I}$  and  $V_{s1-II}, I_{s1-II}$ : pre-fault positive sequence voltage and current at ends  $r_I$  and  $s_{II}$ , respectively;

$Z_{sr1-I}, Z_{sr1-II}$ : equivalent positive sequence series impedance of the line circuits I and II;

$Y_{sr1-I}, Y_{sr1-II}$ : equivalent positive sequence shunt admittance of the line circuits I and II.

The equivalent line parameters are expressed based on the distributed parameter model, considering (11) and (12)

$$Z_{sr-I} = Z_{sr-II} = Z_{c1} \sinh(\gamma_{c1}l) \quad (17)$$

$$Y_{sr-I} = Y_{sr-II} = (2/Z_{c1}) \tanh(\gamma_{c1}l/2) \quad (18)$$

where  $l$  is the length of the line in miles or kilometres.

Based on Fig. 4 and taking measurements at the line end  $s_I$  as reference, we derive the following equations

$$V_{r1-I} = V_{s1-I}(1 + (Y_{sr1-I}/2)Z_{sr1-I}) - I_{s1-I}Z_{sr1-I} \quad (19)$$

$$V_{s1-II} = V_{r1-II}e^{j\delta_v}(1 + (Y_{sr1-II}/2)Z_{sr1-II}) - I_{r1-II}e^{j\delta_i}Z_{sr1-II} \quad (20)$$

where  $\delta_v$  and  $\delta_i$  are synchronisation angles between the two voltage and current phasors at ends  $s_I$  and  $r_{II}$ , respectively, which represent any possible synchronisation error.

The two circuits of the line in Fig. 4 have the same voltage at both terminals s and r. Thus

$$V_{r1-I} = V_{r1-II}e^{j\delta_i}, \quad V_{s1-II} = V_{s1-I} \quad (21)$$

Combining (19)–(21), we compute the synchronisation angles  $\delta_v$  and  $\delta_i$  as follows

$$\delta_v = \arg((V_{s1-I}(1 + (Y_{sr1-I}/2)Z_{sr1-I}) - I_{s1-I}Z_{sr1-I})/V_{r1-II}) \quad (22)$$

$$\delta_i = \arg((V_{r1-II}e^{j\delta_i}(1 + (Y_{sr1-II}/2)Z_{sr1-II}) - V_{s1-I})/(I_{r1-II}Z_{sr1-II})) \quad (23)$$

### 3.3 Faulted circuit selection

The selection of the faulted line circuit can be made by substituting in (19) and (20) the positive sequence voltage and current phasors preceding the fault with those existing during the fault as follows

$$V_{rf1-I,c} = V_{sf1-I}(1 + (Y_{sr1-I}/2)Z_{sr1-I}) - I_{sf1-I}Z_{sr1-I} \quad (24)$$

$$V_{sf1-II,c} = V_{rf1-II}e^{j\delta_v}(1 + (Y_{sr1-II}/2)Z_{sr1-II}) - I_{rf1-II}e^{j\delta_i}Z_{sr1-II} \quad (25)$$

where  $V_{sf1-I}, I_{sf1-I}$  and  $V_{rf1-II}, I_{rf1-II}$  are the positive sequence voltage and current during the fault at measuring

ends  $s_I$  and  $r_{II}$ , respectively;  $V_{sf1_{II,c}}$ ,  $V_{rf1_{I,c}}$  are the calculated positive sequence voltages during the fault at ends  $s_{II}$  and  $r_I$ , respectively.

For the voltages at terminals s and r, we have

$$V_{rf1_{I,m}} = V_{rf1_{II}} e^{j\delta_v}, \quad V_{sf1_{II,m}} = V_{sf1_{I}} \quad (26)$$

where  $V_{sf1_{II,m}}$ ,  $V_{rf1_{I,m}}$  are the positive sequence voltages during the fault at the unmeasured ends  $s_{II}$  and  $r_I$ .

Using (24)–(26), we define the following differentials

$$\Delta V_{rf1_{I}} = |V_{rf1_{I,m}} - V_{rf1_{I,c}}| \quad (27)$$

$$\Delta V_{sf1_{II}} = |V_{sf1_{II,m}} - V_{sf1_{II,c}}| \quad (28)$$

If we assume that the fault lays in circuit I, we obtain

$$\Delta V_{rf1_{I}} \gg 0 \quad \text{and} \quad \Delta V_{sf1_{II}} \simeq 0 \quad (29)$$

Thus, the criterion for minimum differential,  $\min(\Delta V_{rf1_{I}}, \Delta V_{sf1_{II}})$ , indicates the ‘sound’ circuit of the line. It is also clear that when  $\Delta V_{rf1_{I}} \gg 0$  and  $\Delta V_{sf1_{II}} \gg 0$ , an inter-circuit fault has occurred.

### 3.4 Fault location estimation

Based on the analysis of Section 2 and Fig. 5, the fault distance can be estimated in two steps. At first, the voltage and current at the fault point in all sequence networks, shown in Fig. 5, are expressed in terms of those at the two measuring ends and the distance to fault. Afterwards, the fault location is calculated based on the fault boundary condition, which corresponds to the existing fault type, by an iterative method.

In Fig. 5, the following nomenclature is adopted for convenience:

$V_{sf1_{I}}$ ,  $I_{sf1_{I}}$ ,  $V_{sf2_{I}}$ ,  $I_{sf2_{I}}$  and  $V_{rf1_{II}}$ ,  $I_{rf1_{II}}$ ,  $V_{rf2_{II}}$ ,  $I_{rf2_{II}}$ : positive and negative sequence voltages and currents during the fault at measuring ends  $s_I$  and  $r_{II}$ , respectively;

$V_{sf1_{II}}$ ,  $I_{sf1_{II}}$ ,  $V_{sf2_{II}}$ ,  $I_{sf2_{II}}$  and  $V_{rf1_{I}}$ ,  $I_{rf1_{I}}$ ,  $V_{rf2_{I}}$ ,  $I_{rf2_{I}}$ : positive and negative sequence voltages and currents during the fault at ends  $s_{II}$  and  $r_I$ , respectively;

$V_{sf0c}$ ,  $I_{sf0c}$ ,  $V_{rf0c}$ ,  $I_{rf0c}$ : common zero-sequence voltages and currents during the fault at terminals s and r, respectively;

$V_{sf0d}$ ,  $I_{sf0d}$ ,  $V_{rf0d}$ ,  $I_{rf0d}$ : differential zero-sequence voltages and currents during the fault at terminals s and r, respectively;

$Z_{sf1_{I}}$ ,  $Z_{sf1_{II}}$ : equivalent positive sequence series impedance of the line section sf for circuits I and II, respectively;

$Z_{rf1_{I}}$ ,  $Z_{rf1_{II}}$ : equivalent positive sequence series impedance of the line section rf for circuits I and II, respectively;

$Z_{sf0c}$ ,  $Z_{sf0d}$ : equivalent common and differential zero-sequence series impedance of the line section sf, respectively;

$Z_{rf0c}$ ,  $Z_{rf0d}$ : equivalent common and differential zero-sequence series impedance of the line section rf, respectively;

$Y_{sf1_{I}}$ ,  $Y_{sf1_{II}}$ : equivalent positive sequence shunt admittance of the line section sf for circuits I and II, respectively;

$Y_{rf1_{I}}$ ,  $Y_{rf1_{II}}$ : equivalent positive sequence shunt admittance of the line section rf for circuits I and II, respectively;

$Y_{sf0c}$ ,  $Y_{sf0d}$ : equivalent common and differential zero-sequence shunt admittance of the line section sf, respectively;

$Y_{rf0c}$ ,  $Y_{rf0d}$ : equivalent common and differential zero-sequence shunt admittance of the line section rf, respectively;

The equivalent line parameters are expressed based on the distributed parameter model, considering (11)–(16)

$$Z_{sf1_{-j}} = Z_{c1} \sinh(\gamma_{c1} xl) \quad (30)$$

$$Y_{sf1_{-j}} = (2/Z_{c1}) \tanh(\gamma_{c1} xl/2) \quad (31)$$

$$Z_{rf1_{-j}} = Z_{c1} \sinh(\gamma_{c1} (1-x)l) \quad (32)$$

$$Y_{rf1_{-j}} = (2/Z_{c1}) \tanh(\gamma_{c1} (1-x)l/2) \quad (33)$$

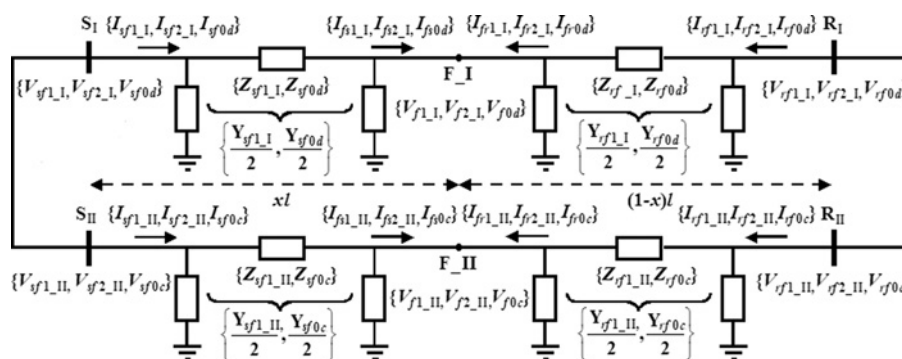


Figure 5 Equivalent PI circuit of decoupled sequence networks

$$Z_{sf0p} = Z_{c0p} \sinh(\gamma_{c0p}xl) \quad (34)$$

$$Y_{sf0p} = (2/Z_{c0p}) \tanh(\gamma_{c0p}xl/2) \quad (35)$$

$$Z_{rf0p} = Z_{c0p} \sinh(\gamma_{c0p}(1-x)l) \quad (36)$$

$$Y_{rf0p} = (2/Z_{c0p}) \tanh(\gamma_{c0p}(1-x)l/2) \quad (37)$$

where  $x$  is the per-unit distance to fault from reference terminal  $s$ ;  $j = I, II$ , representing the circuits I and II of the line and  $p = d, c$ , standing for the differential and common sequence component.

### 3.4.1 Sequence voltage and currents at fault point F:

The objective is to express the sequence voltages and currents at the fault point with respect to the known sequence voltages and currents at ends  $s_I$  and  $r_{II}$  and the unknown distance to fault. The sequence voltages and currents at ends  $s_{II}$  and  $r_I$  are unknown variables, which, if needed, can be easily solved as a function of the known ones and the distance to fault via basic network equations which are valid for the double-circuit line during the fault.

Based on Fig. 5, we can derive the following equations for the positive and negative sequence voltages and currents at fault point F in circuits I and II of the line

$$V_{fk-I} = V_{sfk-I}(1 + (Y_{sf1-I}/2)Z_{sf1-I}) - I_{sfk-I}Z_{sf1-I} \quad (38)$$

$$I_{fsk-I} = (V_{sfk-I} - V_{fk-I})/Z_{sf1-I} - V_{fk-I}(Y_{sf1-I}/2) \quad (39)$$

$$I_{frk-I} = (V_{frk-I} - V_{fk-I})/Z_{rf1-I} - V_{fk-I}(Y_{rf1-I}/2) \quad (40)$$

$$I_{fk-I} = I_{fsk-I} + I_{frk-I} \quad (41)$$

$$V_{fk-II} = V_{rfk-II}e^{j\delta_v}(1 + (Y_{rf1-II}/2)Z_{rf1-II}) - I_{rfk-II}e^{j\delta_i}Z_{rf1-II} \quad (42)$$

$$I_{fsk-II} = (V_{rfk-II} - V_{fk-II})/Z_{rf1-II} - V_{fk-II}(Y_{rf1-II}/2) \quad (43)$$

$$I_{frk-II} = (V_{frk-II}e^{j\delta_v} - V_{fk-II})/Z_{rf1-II} - V_{fk-II}(Y_{rf1-II}/2) \quad (44)$$

$$I_{fk-II} = I_{fsk-II} + I_{frk-II} \quad (45)$$

where  $k = 1, 2$ , denoting the positive and negative sequence component, respectively.

Equations (40) and (43) contain the unknown variables  $V_{rfk-I}$  and  $V_{sfk-II}$  which, however, can be calculated via the measurements at ends  $r_{II}$  and  $s_I$ , respectively, and are given by

$$V_{rfk-I} = V_{rfk-II}e^{j\delta_v} \quad (46)$$

$$V_{sfk-II} = V_{sfk-I} \quad (47)$$

The differential and common sequence voltages and currents

at fault point F are acquired as

$$\begin{aligned} V_{f0p} &= V_{sf0p}(1 + (Y_{sf0p}/2)Z_{sf0p}) - I_{sf0p}Z_{sf0p} \\ &= V_{rf0p}(1 + (Y_{rf0p}/2)Z_{rf0p}) - I_{rf0p}Z_{rf0p} \end{aligned} \quad (48)$$

$$I_{fs0p} = I_{sf0p}(1 + (Y_{sf0p}/2)Z_{sf0p}) - V_{sf0p}(Y_{sf0p} + Z_{sf0p}(Y_{sf0p}/2)^2) \quad (49)$$

$$I_{fr0p} = I_{rf0p}(1 + (Y_{rf0p}/2)Z_{rf0p}) - V_{rf0p}(Y_{rf0p} + Z_{rf0p}(Y_{rf0p}/2)^2) \quad (50)$$

where  $p = d, c$ .

Employing (48)–(50) and (9), (10), we obtain the zero-sequence voltages and currents at fault point F for circuits I and II of the line as

$$V_{fs0-I} = V_{sf0-I}A_{sf0} - I_{sf0-I}B_{sf0} + V_{sf0-II}C_{sf0} - I_{sf0-II}D_{sf0} \quad (51)$$

$$I_{fs0-I} = I_{sf0-I}A_{sf0} - V_{sf0-I}E_{sf0} + I_{sf0-II}C_{sf0} - V_{sf0-II}F_{sf0} \quad (52)$$

$$\begin{aligned} V_{fr0-I} &= V_{rf0-I}A_{rf0} - I_{rf0-I}B_{rf0} + V_{rf0-II}e^{j\delta_v}C_{rf0} \\ &\quad - I_{rf0-II}e^{j\delta_i}D_{rf0} \end{aligned} \quad (53)$$

$$\begin{aligned} I_{fr0-I} &= I_{rf0-I}A_{rf0} - V_{rf0-I}E_{rf0} + I_{rf0-II}e^{j\delta_i}C_{rf0} \\ &\quad - V_{rf0-II}e^{j\delta_v}F_{rf0} \end{aligned} \quad (54)$$

$$I_{f0-I} = I_{fs0-I} + I_{fr0-I} \quad (55)$$

$$V_{fs0-II} = V_{sf0-I}C_{sf0} - I_{sf0-I}D_{sf0} + V_{sf0-II}A_{sf0} - I_{sf0-II}B_{sf0} \quad (56)$$

$$I_{fs0-II} = I_{sf0-I}C_{sf0} - V_{sf0-I}F_{sf0} + I_{sf0-II}A_{sf0} - V_{sf0-II}E_{sf0} \quad (57)$$

$$\begin{aligned} V_{fr0-II} &= V_{rf0-I}C_{rf0} - I_{rf0-I}D_{rf0} + V_{rf0-II}e^{j\delta_v}A_{rf0} \\ &\quad - I_{rf0-II}e^{j\delta_i}B_{rf0} \end{aligned} \quad (58)$$

$$\begin{aligned} I_{fr0-II} &= I_{rf0-I}C_{rf0} - V_{rf0-I}F_{rf0} + I_{rf0-II}e^{j\delta_i}A_{rf0} \\ &\quad - V_{rf0-II}e^{j\delta_v}E_{rf0} \end{aligned} \quad (59)$$

$$I_{f0-II} = I_{fs0-II} + I_{fr0-II} \quad (60)$$

where  $A_{sf0}, B_{sf0}, C_{sf0}, D_{sf0}, E_{sf0}, F_{sf0}$  and  $A_{rf0}, B_{rf0}, C_{rf0}, D_{rf0}, E_{rf0}, F_{rf0}$  are the equivalent parameters of the zero-sequence network defined in Appendix.

Moreover, the two circuits have the same zero-sequence voltage at both line terminals  $s$  and  $r$ , thus

$$V_{rf0-I} = V_{rf0-II}e^{j\delta_v} \quad (61)$$

$$V_{sf0-II} = V_{sf0-I} \quad (62)$$

From (38)–(47), it is clear that the positive and negative sequence voltages and currents at fault point F can be obtained as a straightforward function of the unknown fault distance  $x$  and the known voltages  $V_{sfk\_I}$ ,  $V_{rfk\_II}$  and currents  $I_{sfk\_I}$ ,  $I_{rfk\_II}$  at ends  $s_I$  and  $r_{II}$ , respectively. The same does not hold true for zero-sequence voltages and currents, which are also dependent on the unknown variables  $I_{sf0\_II}$  and  $I_{rf0\_I}$ . To eliminate the two unknown variables from (51)–(60), we can solve the following  $2 \times 2$  linear system which reflects the zero-sequence network constraint equations that exist in the double-circuit line during a fault involving ground

$$\begin{bmatrix} a & b \\ c & d \end{bmatrix} \begin{bmatrix} I_{sf0\_II} \\ I_{rf0\_I} \end{bmatrix} = \begin{bmatrix} e \\ f \end{bmatrix} \Rightarrow \begin{bmatrix} I_{sf0\_II} \\ I_{rf0\_I} \end{bmatrix} = \begin{bmatrix} a & b \\ c & d \end{bmatrix}^{-1} \begin{bmatrix} e \\ f \end{bmatrix} \quad (63)$$

where  $a, b, c, d, e, f$  are the coefficients dependent on the ground fault condition, given in Table 4 of the Appendix.

Substituting the solution of (63) in (51)–(54) and (56)–(59), respectively, yields the zero-sequence voltages and currents at fault point F of circuits I and II, as a function of the known zero-sequence variables at ends  $s_I$  and  $r_{II}$  and the fault distance.

**3.4.2 Theory of fault location:** In the fault state, different fault types give rise to different boundary conditions. The fault boundary conditions can be expressed in terms of the fault voltage  $V_f$ , the fault current  $I_f$  and the fault resistance  $R_f$

$$V_f = R_f I_f \quad (64)$$

In (64), fault resistance  $R_f$  is unknown. Fault voltage  $V_f$  can be calculated by the six-sequence voltages  $V_{fk\_I}$ ,  $V_{fk\_II}$ , where  $k = 0, 1, 2$ , corresponding to (38), (42), (51) and (56), which themselves can be expressed by the known voltages  $V_{sfk\_I}$ ,  $V_{rfk\_II}$  and currents  $I_{sfk\_I}$ ,  $I_{rfk\_II}$  at ends  $s_I$  and  $r_{II}$ , respectively. Thus, the fault voltage  $V_f$  can be written as

$$V_f(x) = f(V_{sfk\_I}, V_{rfk\_II}, I_{sfk\_I}, I_{rfk\_II}, x) \quad (65)$$

In (65), only the fault distance  $x$  is unknown. Similarly to (65), the fault current  $I_f$  can be written as

$$I_f(x) = g(V_{sfk\_I}, V_{rfk\_II}, I_{sfk\_I}, I_{rfk\_II}, x) \quad (66)$$

According to (64)–(66),  $V_f = R_f I_f$  can be transformed into fault locating equation

$$F(x) = \text{Im} \left\{ \frac{V_f(x)}{I_f(x)} \right\} = \text{Im} \left\{ \frac{f(V_{sfk\_I}, V_{rfk\_II}, I_{sfk\_I}, I_{rfk\_II}, x)}{g(V_{sfk\_I}, V_{rfk\_II}, I_{sfk\_I}, I_{rfk\_II}, x)} \right\} = 0 \quad (67)$$

where  $\text{Im}$  denotes the imaginary part.

Since the fault location equation is non-linear, a numerical method is needed to obtain the solution of  $x$ . The well-known Newton–Raphson method, which computes the correction  $\Delta x_v$  at each iteration, can be employed

$$\Delta x_v = -\frac{F(x_v)}{F'(x_v)} \quad (68)$$

where  $v = 0, 1, 2, \dots$  is the iteration count,  $\Delta x_v = x_{v+1} - x_v$  and  $F'(x_v) = dF(x_v)/dx$  is the derivative of  $F(x)$  at the  $v$ th iteration. The iterative process converges when the correction update becomes less than a specified tolerance.

**3.4.3 Performance equations for various fault types:** The proposed algorithm can deal with all possible fault types encountered on double-circuit lines. These fault types can be divided into two categories. One is faults within a single circuit, which includes IAG, IBC, IBCG, IABC, and so on. The other is faults between circuits, called inter-circuit or cross-country faults, which includes IAIIBG, IAIIBCG, IBCIICG, IABIIBC, IABCIIAB, and so on. The stars of fault resistances shown in Fig. 6 allows to represent any type of fault eliminating, when necessary, those legs that are not involved in the fault type considered [20]. For instance, the inter-circuit fault IAIIBG is reflected when the legs containing the resistances  $R_{faI}$ ,  $R_{fbII}$  and  $R_g$  are maintained and the rest are neglected.

The performance equations for an IAG and an IAIIBG fault, which have the most probability among single-circuit and inter-circuit faults, are developed below and the equations for other fault types can be deduced from these two basic types.

*Performance equations for faults within a single-circuit:* The boundary condition for a single phase-to-ground fault IAG can be derived from Fig. 6. It is

$$V_{faI} = I_{faI} R_f \quad (69)$$

where  $V_{faI} = V_{f1I} + V_{f2I} + V_{f0I}$  is the fault voltage,  $I_{faI} = I_{f1I} + I_{f2I} + I_{f0I}$  is the fault current and  $R_f = R_{faI} + R_g$  is the total fault resistance. This fault type involves a ground fault condition in circuit I. Thus, we use the values of  $a, b, c, d, e, f$  in the first column of Table 4 in order to determine the unknown variables  $I_{sf0\_II}$

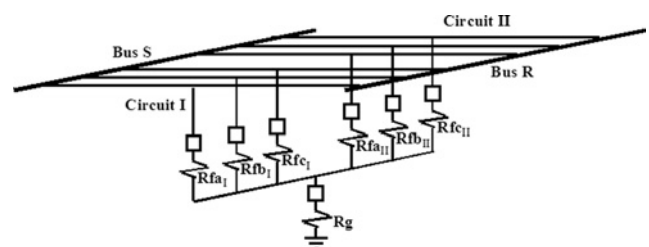


Figure 6 Fault resistances at the fault point

and  $I_{f0\_I}$ . Afterwards, using (38)–(41), (46), (51)–(55), (61) and (62), the fault location equation in (67) is written as (see (70))

Then, (70) can be solved for the fault distance, which is the only unknown parameter. In a similar manner, we can derive the fault locating equations for other types of faults occurring within a single circuit.

*Performance equations for faults between circuits:* The boundary conditions for an inter-circuit fault IAIIBG can also be derived from Fig. 6. They are

$$V_{fa\_I} - I_{fa\_I}R_{fa\_I} = (I_{fa\_I} + I_{fb\_II})R_g \quad (71)$$

$$V_{fa\_I} - I_{fa\_I}R_{fa\_I} = V_{fb\_II} - I_{fb\_II}R_{fb\_II} \quad (72)$$

where  $V_{fb\_II} = a^2V_{f1\_II} + aV_{f2\_II} + V_{f0\_II}$  and  $I_{fb\_II} = a^2I_{f1\_II} + aI_{f2\_II} + I_{f0\_II}$  are the fault voltage and current at circuit II. Using the real and imaginary parts of (72), the unknown resistance  $R_{fa\_I}$  can be expressed in terms of the fault voltages and currents in both circuits, as follows

$$R_{fa\_I} = \frac{\text{Re}\{I_{fb\_II}\}\text{Im}\{V_{fa\_I} - V_{fb\_II}\} - \text{Im}\{I_{fb\_II}\}\text{Re}\{V_{fa\_I} - V_{fb\_II}\}}{\text{Re}\{I_{fb\_II}\}\text{Im}\{I_{fa\_I}\} - \text{Im}\{I_{fb\_II}\}\text{Re}\{I_{fa\_I}\}} \quad (73)$$

Moreover, since this type of fault involves a ground fault condition in both circuits of the double-circuit line, we use the values of  $a, b, c, d, e, f$  in the third column of Table 4 in order to obtain the unknown variables  $I_{sf0\_II}$  and  $I_{f0\_I}$ . Afterwards, using (38)–(47), (51)–(62) and (73), the fault location in (67) is written as (see (74))

Then, (74) can be solved for the fault distance, which is the only unknown parameter. In similar manner, the fault locating equations for other types of faults occurring between circuits can be readily derived.

## 4 Fault location performance evaluation studies

This section presents test results based on ATP-EMTP simulations to verify the accuracy of the proposed

algorithm. A 400-kV power network (Fig. 3) including a double-circuit transmission line has been used. Network and line parameters are given in Table 1. The double-circuit line is represented by Clarke’s distributed parameter line model. The ATP network model includes both the voltage and current transformers, VTs and CTs, at the two measuring ends of the line, which have been intentionally modelled as errorless transforming devices in order to show the errors of the presented algorithm itself.

The fault location algorithm has been developed in MATLAB. The analogue filters, needed for removing noise from the voltage and current signals obtained by ATP-EMTP, are implemented using a fourth-order Butterworth filter with cut-off frequency equal to 500 Hz. Then, the phase voltage and current phasors are

**Table 1** Parameters of the 400 kV transmission network

Components	Parameters	
transmission line data	$L$	300 km
	$Z_1$	$0.0276 + j0.3151 \Omega/\text{km}$
	$B_1$	$4.0841 \mu\text{S}/\text{km}$
	$Z_0$	$0.2680 + j1.0371 \Omega/\text{km}$
	$B_0$	$2.7018 \mu\text{S}/\text{km}$
	$Z_{0M}$	$0.2300 + j0.6308 \Omega/\text{km}$
	$B_{0M}$	$1.6242 \mu\text{S}/\text{km}$
equivalent system at terminal s	$Z_{s1}$	$1.312 + j15.0 \Omega$
	$Z_{s0}$	$2.334 + j26.6 \Omega$
	magnitude of $E_s$	1 (p.u.)
	angle of $E_s$	$0^\circ$
equivalent system at terminal r	$Z_{r1}$	$2Z_{s1}$
	$Z_{r0}$	$2Z_{s0}$
	magnitude of $E_r$	0.99 (p.u.)
	angle of $E_r$	$-30^\circ$

$$\text{Im}\left(\frac{V_f(x)}{I_f(x)}\right) = \text{Im}\left(\frac{V_{fa\_I}}{I_{fa\_I}}\right) = \text{Im}\left(\frac{f(V_{sf1\_I}, V_{rf1\_II}, I_{sf1\_I}, V_{sf2\_I}, V_{rf2\_II}, I_{sf2\_I}, V_{sf0\_I}, V_{rf0\_II}, I_{sf0\_I}, I_{rf0\_II}, x)}{g(V_{sf1\_I}, V_{rf1\_II}, I_{sf1\_I}, V_{sf2\_I}, V_{rf2\_II}, I_{sf2\_I}, V_{sf0\_I}, V_{rf0\_II}, I_{sf0\_I}, I_{rf0\_II}, x)}\right) = 0 \quad (70)$$

$$\begin{aligned} \text{Im}\left(\frac{V_f(x)}{I_f(x)}\right) &= \text{Im}\left(\frac{V_{fa\_I} - I_{fa\_I}R_{fa\_I}}{I_{fa\_I} + I_{fb\_II}}\right) \\ &= \text{Im}\left(\frac{f(V_{sf1\_I}, V_{rf1\_II}, I_{sf1\_I}, I_{rf1\_II}, V_{sf2\_I}, V_{rf2\_II}, I_{sf2\_I}, I_{rf2\_II}, V_{sf0\_I}, V_{rf0\_II}, I_{sf0\_I}, I_{rf0\_II}, x)}{g(V_{sf1\_I}, V_{rf1\_II}, I_{sf1\_I}, I_{rf1\_II}, V_{sf2\_I}, V_{rf2\_II}, I_{sf2\_I}, I_{rf2\_II}, V_{sf0\_I}, V_{rf0\_II}, I_{sf0\_I}, I_{rf0\_II}, x)}\right) = 0 \end{aligned} \quad (74)$$

extracted using the DFT algorithm working with 20 samples per cycle. Finally, the symmetrical component transformation is applied to calculate the positive, negative and zero-sequence voltage and current phasors at the two measuring ends.

After the phasor estimation process, the fault-type detection algorithm is applied to determine the phases involved in the fault. Within this process, the fault data generated by ATP-EMTP simulations are divided into pre-fault and fault segments for further manipulation. The part of the algorithm that is assigned with data alignment is not executed, since the data obtained from ATP-EMTP are already time-aligned. Next, the algorithms for synchronisation error determination and faulted circuit selection are executed using pre-fault and fault data, respectively. At last, the results of fault location estimation algorithm are provided.

A large number of simulations for different fault types have been carried out for various fault resistances and fault distances. To simulate synchronisation errors, the calculated voltage and current phasors at line end  $r_{II}$  have been rotated by  $18^\circ$  and  $9^\circ$ , respectively, in all test cases. To estimate the distance to fault  $x$ , the iteration process is

terminated when its update becomes less than  $10^{-6}$ . The initial value  $x_0$  adopted for the fault location estimation is 0.5 p.u.

In all test cases, the proposed algorithm shows an excellent performance, making correct decisions for the fault type and the faulted circuit and giving highly precise estimates for the synchronisation angles. Moreover, the fault location estimation algorithm reached convergence within six iterations for most cases. Table 2 presents the fault location results for four different types of single-circuit faults and six different types of inter-circuit faults. The fault location errors given in the table are calculated from

$$\text{error} = \frac{|\text{actual fault distance} - \text{calculated fault distance}|}{\text{total line length}} \times 100\% \quad (75)$$

It is clear that the maximum error in Table 2 is less than 0.2%, which confirms that the fault location algorithm has very high accuracy. Table 2 also shows that the fault resistance and fault distance have little influence on the fault location accuracy. To further investigate the influence by fault resistances and coupling effects, more simulation

**Table 2** Fault locating results of a 400 kV double-circuit transmission line (source s leading source r by  $30^\circ$ )

Fault types	Fault resistance, $\Omega$							50, km		100, km		150, km		200, km		250, km	
	$R_{fal}$	$R_{fbl}$	$R_{fcl}$	$R_{fall}$	$R_{fbll}$	$R_{fcil}$	$R_g$	Result, km	Error, %	Result, km	Error, %	Result, km	Error, %	Result, km	Error, %	Result, km	Error, %
IAG	0						10	49.987	0.0043	100.027	0.0089	150.059	0.0197	200.079	0.0264	250.305	0.1015
IIBC					1	1		49.966	0.0113	100.033	0.0111	150.053	0.0176	200.040	0.0133	250.046	0.0153
IBCG		0.5	0.5				4	49.986	0.0047	99.914	0.0286	149.873	0.0425	199.787	0.0712	249.797	0.0678
IIBC				0.5	0.5	0.5		49.451	0.1829	99.548	0.1507	149.906	0.0312	199.915	0.0283	250.053	0.0178
IAIIBCG	1				0.5	0.5	10	50.078	0.0260	99.9553	0.0149	149.997	0.0009	199.992	0.0028	250.008	0.0026
IAIIBG	0.5				1		10	50.047	0.0157	100.125	0.0418	150.089	0.0297	200.335	0.1118	249.903	0.0325
IBCIIBG		0.5	0.5		1		10	50.041	0.0047	100.020	0.0067	150.033	0.0111	200.055	0.0185	250.067	0.0224
ICAIICA	0.5		0.5	0.5		0.5		50.000	0.0001	99.906	0.0314	149.910	0.0300	200.015	0.0050	250.088	0.0293
IABCIIBCG	0.25	0.25	0.25		0.5	0.5	10	49.995	0.0017	99.994	0.0019	149.985	0.0051	199.963	0.0123	250.007	0.0025
IABIICAG	0.5	0.5		1		1	10	50.004	0.0013	99.998	0.0006	150.005	0.0018	200.004	0.0014	249.976	0.0081
IAG	0						100	49.904	0.0320	99.919	0.0271	150.052	0.0173	200.450	0.1501	250.556	0.1854
IIBC					2.5	2.5		49.946	0.0180	99.972	0.0095	149.987	0.0042	199.998	0.0007	250.016	0.0052
IBCG		2.5	2.5				35	49.936	0.0021	99.989	0.0034	149.998	0.0005	199.996	0.0015	250.091	0.0302
IIBC				1	1	1		49.546	0.1512	99.548	0.1507	149.899	0.0337	199.928	0.0283	250.039	0.0131
IAIIBCG	2				1	1	100	50.387	0.1290	100.593	0.1978	150.007	0.0002	200.497	0.1655	250.344	0.1145
IAIIBG	1				2		100	50.050	0.0168	100.079	0.0263	150.051	0.0170	200.118	0.0392	249.962	0.0126
IBCIIBG		1	1		2		100	50.007	0.0023	100.019	0.0063	150.026	0.0087	200.049	0.0166	250.268	0.0889
ICAIICA	1		1	1		1		49.999	0.0002	99.965	0.0116	149.942	0.0192	200.009	0.0030	250.067	0.0223
IABCIIBCG	0.5	0.5	0.5		1	1	100	50.032	0.0105	100.003	0.0011	150.008	0.0027	200.011	0.0036	249.935	0.0215
IABIICAG	1	1		2		2	100	49.994	0.0019	99.994	0.0019	150.005	0.0015	200.013	0.0043	249.980	0.0069

**Table 3** Fault locating results of a 400 kV double-circuit transmission line (source s leading source r by 45°)

Fault types	Fault resistance, $\Omega$							50, km		100, km		150, km		200, km		250, km	
	$R_{fal}$	$R_{fbl}$	$R_{fcl}$	$R_{fall}$	$R_{fbll}$	$R_{fcil}$	$R_g$	Result, km	Error, %	Result, km	Error, %	Result, km	Error, %	Result, km	Error, %	Result, km	Error, %
IAG	0						0	49.987	0.0042	100.027	0.0090	150.033	0.0109	200.069	0.0231	250.057	0.0189
	0						100	49.932	0.0227	99.933	0.0222	150.050	0.0167	200.397	0.1322	250.632	0.2107
	0						250	49.936	0.0222	99.921	0.0264	150.137	0.0457	200.728	0.2426	248.967	0.3445
	0						500	50.040	0.0134	99.989	0.0036	150.313	0.1042	201.138	0.3793	251.417	0.4724
IBIICG		0.5				0.5	0	50.055	0.0018	100.046	0.0153	150.265	0.0882	200.750	0.2501	249.856	0.0479
		0.5				0.5	100	50.043	0.0144	100.041	0.0137	150.116	0.0386	200.171	0.0570	250.144	0.0479
		1				1	250	50.035	0.0012	100.043	0.0108	150.131	0.0436	200.848	0.2875	249.479	0.1737
		1				1	500	50.039	0.0131	100.039	0.0130	150.175	0.0582	198.837	0.3867	250.935	0.3115

cases are given in Table 3. In this table, simulated fault types are IAG and IBIICG, which are the most possible to occur among single-circuit and inter-circuit faults, respectively. The fault resistances are assumed from 0 to 500  $\Omega$ , and the coupling effects are considered through the pre-fault load current by making the phase angle of source s leading source r by 45°. Table 3 shows that the fault resistance and coupling effects have very little influence on the fault location accuracy.

## 5 Conclusion

A new algorithm for locating faults in double-circuit lines utilising a limited number of unsynchronised voltage and current measurements at two anti-parallel ends of the line has been presented. The algorithm is based on distributed parameter line model with use of a modal transformation matrix, which decouples the mutually coupled zero-sequence networks. Thus, it achieves superior accuracy especially for long transmission lines. The algorithm can deal effectively with all possible fault types encountered in double-circuit line arrangements, including both single-circuit and inter-circuit faults. Moreover, the algorithm is insensitive to fault resistances, load currents and source impedances. The validity of the algorithm has been verified by extended EMTP simulations. All applied tests reveal a high accuracy and promising performance for all situations.

## 6 References

- [1] LIAO Y., ELANGOVA S.: 'Digital distance relaying algorithm for first-zone protection for parallel transmission lines', *IEE Proc. Gener., Transm., Distrib.*, 1998, **145**, (5), pp. 531–536
- [2] QINGCHAO Z., YAO Z., WENNAN S., YIXIN Y., ZHIGANG W.: 'Fault location of two-parallel transmission line for non-earth fault using one-terminal data', *IEEE Trans. Power Deliv.*, 1998, **14**, (3), pp. 863–867
- [3] SHENG L.B., ELANGOVA S.: 'A fault location method for parallel transmission lines', *Electr. Power Energy Syst.*, 1999, **21**, (4), pp. 253–259
- [4] AHN Y., CHOI M., KANG S.: 'An accurate fault location algorithm for double-circuit transmission systems'. IEEE Power Engineering Society Meeting, Seattle, July 2000, vol. 3, pp. 1344–1349
- [5] KAWADY T., STENZEL J.: 'A practical fault location approach for double circuit transmission lines using single end data', *IEEE Trans. Power Deliv.*, 2003, **18**, (4), pp. 1166–1173
- [6] IZYKOWSKI J., ROSOŁOWSKI E., SAHA M.M.: 'Locating faults in parallel transmission lines under availability of complete measurements at one end', *IEE Proc. Gener., Transm., Distrib.*, 2004, **151**, (2), pp. 268–273
- [7] SONG G., SUONAN J., GE Y.: 'An accurate fault location algorithm for parallel transmission lines using one-terminal data', *Electr. Power Energy Syst.*, 2009, **31**, (2–3), pp. 124–129
- [8] JOHNS A.T., JAMALI S.: 'Accurate fault location technique for power transmission lines', *IEE Proc. Gener., Transm., Distrib.*, 1990, **137**, (6), pp. 395–402
- [9] FUNABASHI T., OTOGURO H., MIZUMA Y., DUBE L., AMETANI A.: 'Digital fault location for parallel double-circuit multi-terminal transmission lines', *IEEE Trans. Power Deliv.*, 2000, **15**, (2), pp. 531–537
- [10] SONG G., SUONAN J., XU Q., CHEN P., GE Y.: 'Parallel transmission lines fault location algorithm based on differential component net', *IEEE Trans. Power Deliv.*, 2005, **20**, (4), pp. 2396–2406
- [11] SUONAN J., SONG G., XU Q., CHAO Q.: 'Time-domain fault location for parallel transmission lines using unsynchronized currents', *Electr. Power Energy Syst.*, 2006, **28**, (4), pp. 253–260

[12] LIEN K.-P., LIU C.-W., YU C.-S., JIANG J.-A.: 'Transmission network fault location observability with minimal PMU placement', *IEEE Trans. Power Deliv.*, 2006, **21**, (3), pp. 1128–1136

[13] LIAO Y.: 'Equivalent PI circuit for zero-sequence networks of parallel transmission lines', *Electr. Power Comp. Syst.*, 2009, **37**, (7), pp. 787–797

[14] GRAINGER J., STEVENSON W.: 'Power system analysis' (McGraw-Hill Inc., New York, 1994)

[15] WEDEPOHL L.M.: 'Application of matrix methods to the solution of travelling-wave phenomena in polyphase systems', *Proc. Inst. Electr.*, 1963, **110**, (112), pp. 2200–2212

[16] DOMMEL H.W.: 'EMTP theory book' (Microtran Power System Analysis Corp., Vancouver, 1992)

[17] FECTEAU C.: 'Accurate fault location algorithm for series compensated lines using two-terminal unsynchronized measurements and Hydro-Quebec's field experience'. Proc. 33rd Annual Western Protective Relay Conf. (WPRC), Spokane, Washington, 2006, pp. 1–16

[18] IEEE Standard C37.111–1991: 'IEEE Standard Common Format for Transient Data Exchange (COMTRADE) for Power Systems', Version 1.8, February 1991

[19] KASZTENNY B., CAMPBELL B., MAZEREEUW J.: 'Phase selection for single-pole tripping: weak infeed conditions and cross-country faults'. Proc. 27th Annual Western Protective Relay Conf. (WPRC), Spokane, Washington, 2000, pp. 1–19

[20] AGRASAR M., URIONDO F., HERNANDEZ J.R., ALVAREZ R.: 'A useful methodology for analyzing distance relays performance during simple and inter-circuit in multi-circuit lines', *IEEE Trans. Power Deliv.*, 1997, **12**, (4), pp. 1465–1471

## 7 Appendix

The equivalent zero-sequence parameters defined in deducing (51)–(60) are shown as follows

$$A_{gf0} = \frac{1}{2}(2 + (Y_{gf0c}/2)Z_{gf0c} + (Y_{gf0d}/2)Z_{gf0d}) \quad (76)$$

$$B_{gf0} = \frac{1}{2}(Z_{gf0c} + Z_{gf0d}) \quad (77)$$

$$C_{gf0} = \frac{1}{2}((Y_{gf0c}/2)Z_{gf0c} - (Y_{gf0d}/2)Z_{gf0d}) \quad (78)$$

$$D_{gf0} = \frac{1}{2}(Z_{gf0c} - Z_{gf0d}) \quad (79)$$

$$E_{gf0} = \frac{1}{2}((Y_{gf0c} + Z_{gf0c}(Y_{gf0c}/2)^2) + (Y_{gf0d} + Z_{gf0d}(Y_{gf0d}/2)^2)) \quad (80)$$

$$F_{gf0} = \frac{1}{2}((Y_{gf0c} + Z_{gf0c}(Y_{gf0c}/2)^2) - (Y_{gf0d} + Z_{gf0d}(Y_{gf0d}/2)^2)) \quad (81)$$

where  $g = s, r$ , representing the sending  $s$  and receiving  $r$  terminal of the line, respectively.

The coefficients defined in deducing (63) with respect to the ground fault conditions in the double-circuit line are shown in Table 4.

**Table 4** Coefficients used to determine the two unknown currents  $I_{sf0\_II}$  and  $I_{rf0\_I}$

	Faulted circuit I ( $V_{fs0\_II} = V_{fr0\_II}$ and $I_{f0\_II} = 0$ )	Faulted circuit II ( $V_{fs0\_I} = V_{fr0\_I}$ and $I_{f0\_I} = 0$ )	Faulted circuit I and II ( $V_{fs0\_I} = V_{fr0\_I}$ and $V_{fs0\_II} = V_{fr0\_II}$ )
<i>a</i>	$-B_{sf0}$	$-D_{sf0}$	$-D_{sf0}$
<i>b</i>	$D_{rf0}$	$B_{rf0}$	$B_{rf0}$
<i>c</i>	$A_{sf0}$	$C_{sf0}$	$-B_{sf0}$
<i>d</i>	$C_{rf0}$	$A_{rf0}$	$D_{rf0}$
<i>e</i>	$V_{rf0\_I}e^{j\delta_v}(A_{rf0} + C_{rf0}) - I_{rf0\_I}e^{j\delta_i}B_{rf0}$ $- V_{sf0\_I}(A_{sf0} + C_{sf0}) + I_{sf0\_I}D_{sf0}$	$V_{rf0\_II}e^{j\delta_v}(A_{rf0} + C_{rf0}) - I_{rf0\_II}e^{j\delta_i}D_{rf0}$ $- V_{sf0\_II}(A_{sf0} + C_{sf0}) + I_{sf0\_II}B_{sf0}$	$V_{rf0\_II}e^{j\delta_v}(A_{rf0} + C_{rf0}) - I_{rf0\_II}e^{j\delta_i}D_{rf0}$ $- V_{sf0\_II}(A_{sf0} + C_{sf0}) + I_{sf0\_II}B_{sf0}$
<i>f</i>	$V_{sf0\_I}(E_{sf0} + F_{sf0}) - I_{sf0\_I}C_{sf0}$ $+ V_{rf0\_I}e^{j\delta_v}(E_{rf0} + F_{rf0}) - I_{rf0\_I}e^{j\delta_i}A_{rf0}$	$V_{sf0\_II}(E_{sf0} + F_{sf0}) - I_{sf0\_II}A_{sf0}$ $+ V_{rf0\_II}e^{j\delta_v}(E_{rf0} + F_{rf0}) - I_{rf0\_II}e^{j\delta_i}C_{rf0}$	$V_{rf0\_II}e^{j\delta_v}(A_{rf0} + C_{rf0}) - I_{rf0\_II}e^{j\delta_i}B_{rf0}$ $- V_{sf0\_II}(A_{sf0} + C_{sf0}) + I_{sf0\_II}D_{sf0}$